Research Reports of National Institute of Technology, Nagaoka College, Vol. 59, 2024

Paper

Density-based topology optimization for maximally stiff structure problem using Two-phase materials

Takahiko KURAHASHI[1], Sakura ICHIKAWA[2], Masayuki KISHIDA[3,4], Mizuki IKARASHI[5] and Tetsuro IYAMA[6]

[1]Department of Mechanical Engineering, Institute of GIGAKU, Nagaoka University of Technology
[2]Mechanical Engineering, Bachelor's Program, School of Engineering, Nagaoka University of Technology (Current affiliation : OILES CORPORATION)
[3]Department of Mechanical Engineering, National Institute of Technology, Gifu College
[4]Science of Technology Innovation, 5-year Integrated Doctoral Program, Graduate School of Engineering, Nagaoka University of Technology
[5]Mechanical Engineering, Master's Program, Graduate School of Engineering, Nagaoka University of Technology
[6]Department of Mechanical Engineering, National Institute of Technology, Nagaoka College

Herein, we present numerical results obtained after performing density-based topology optimization for a maximally stiff structure problem using two-phase materials. A maximally stiff structure was modeled to minimize the strain energy of the structure. The Young's modulus expressed based on a two-phase material, such as a functionally graded material at the junction point, was used in the density-based topology optimization. The two-phase material was completely separated in the optimized structure, and the strain energies before and after the separation were compared.

Key Words: *Density-based topology optimization, Two-phase material, Maximally stiff structure, Adjoint variable method, Finite element method*

1. Introduction

In recent years, researchers have attempted to use various materials to reduce the weight of automobile components[1)]. Additionally, researchers have begun to use topology optimization technology to manufacture automobile components[2)]. Considering these trends, the topology optimization of two-phase materials[3)] is investigated in this study. In topology optimization analysis using a two-phase material, the Young's modulus is defined by a two-phase material. Owing to topology optimization, a structure in which the Young's modulus varies gradually at the junction point is obtained. However, in automobile manufacturing, separating the material used from the junction point is desirable.

In this study, a topology optimization analysis for a maximally stiff structure is performed, and the value of the performance function is compared before and after the separation of two-phase materials. The performance function is defined by the strain energy, and numerical experiments are performed using the Messerschmitt–Bölkow–Blohm (MBB) model.

2. Formulations for density-based topology optimization problem

The governing equation for the linear elastic deformation is expressed in Eqs. (1)–(3). These equations are written using summation convention.

$$\sigma_{ij,j} = 0 \tag{1}$$

$$\sigma_{ij} = D_{ijkl}\epsilon_{kl} \tag{2}$$

$$\epsilon_{ij} = \frac{1}{2}(u_{i,j} + u_{j,i}) \tag{3}$$

Here, σ_{ij}, ϵ_{ij}, D_{ijkl}, and u_i represent the components of stress and strain tensors, the elasticity coefficient tensor, and the displacement component, respectively. Applying the finite element Galerkin procedure to discretize Eqs. (1)–(3), the finite element equation shown in Eq. (4) is obtained[4]. Here, $\boldsymbol{u}_e$ and $\boldsymbol{f}_e$ are the displacement and external force vectors, respectively; $\boldsymbol{K}_e$ is the stiffness matrix, as expressed in Eq. (5); $\boldsymbol{B}_e$ and $\boldsymbol{D}_e$ denote the B matrix and elasticity coefficient matrix, respectively.

$$\boldsymbol{K}_e\boldsymbol{u}_e = \boldsymbol{f}_e \tag{4}$$

$$\boldsymbol{K}_e = \int_{\Omega_e} \boldsymbol{B}_e^T \boldsymbol{D}_e \boldsymbol{B}_e \, d\Omega \tag{5}$$

Assembling Eq. (4) for all elements, the finite element equation for the entire domain is obtained as shown in Eq. (6). The boundary condition is defined by Eq. (7), where Γ_1 and Γ_2 indicate the Dirichlet and Neumann boundaries, respectively, and the hat symbol indicates the specified value.

$$\boldsymbol{K}\boldsymbol{u} = \boldsymbol{f} \tag{6}$$

$$\begin{cases} \boldsymbol{u} = \hat{\boldsymbol{u}} & \text{on} \quad \Gamma_1 \\ \boldsymbol{f} = \hat{\boldsymbol{f}} & \text{on} \quad \Gamma_2 \end{cases} \tag{7}$$

To solve the maximally stiff structural problem, the performance function is defined as shown in Eq. (8).

$$J = \frac{1}{2}\boldsymbol{u}^T\boldsymbol{f} = \frac{1}{2}\boldsymbol{u}^T\boldsymbol{K}\boldsymbol{u} \tag{8}$$

The problem is to determine the optimal topology to minimize the performance function J. Considering the assembled finite element equation as the constraint condition of the performance function, the performance function extended by the adjoint variable is obtained as shown in Eq. (9), which is known as the Lagrange function.

$$J^* = \frac{1}{2}\left(\boldsymbol{u}^T\boldsymbol{K}(\rho_{1e},\rho_{2e})\boldsymbol{u} + \boldsymbol{\lambda}^T(\boldsymbol{K}(\rho_{1e},\rho_{2e})\boldsymbol{u} - \boldsymbol{f})\right) \tag{9}$$

Meanwhile, Eqs. (10) and (11) are obtained from the stationary condition of the Lagrange function. Eqs. (12) and (13) can be obtained from Eqs. (10) and (11), respectively, and the corresponding equations for the displacement and adjoint variable vectors (Eq. (14) are derived from Eq. (12) and (13), respectively. The relationship derived is known as the self-adjoint relationship.

$$\frac{\partial J^*}{\partial \boldsymbol{\lambda}} = \boldsymbol{K}\boldsymbol{u} - \boldsymbol{f} = \boldsymbol{0} \tag{10}$$

$$\frac{\partial J^*}{\partial \boldsymbol{u}} = \boldsymbol{K}\boldsymbol{u} + \boldsymbol{\lambda}^T\boldsymbol{K} = \boldsymbol{f} + \boldsymbol{K}^T\boldsymbol{\lambda} = \boldsymbol{0} \tag{11}$$

$$\boldsymbol{K}\boldsymbol{u} = \boldsymbol{f} \tag{12}$$

$$\boldsymbol{K}^T\boldsymbol{\lambda} = -\boldsymbol{f} \tag{13}$$

$$\boldsymbol{u} = -\boldsymbol{\lambda} \tag{14}$$

Here, ρ_{1e} and ρ_{2e} are introduced as the design variables, and the Young's modulus E is represented by Eq. (15), where E_0, E_1, E_2, and p indicate the lower limit of the Young's modulus, the Young's modulus for materials A and B, and the penalty parameter, respectively.

$$\begin{aligned} &E(\rho_1,\rho_2) \\ &= \left(\left(1-\rho_2^p\right)E_1 + E_2\rho_2^p\right)\rho_1^p + E_0\left(1-\rho_1^p\right) \\ &= (E_2 - E_1)\rho_1^p\rho_2^p + (E_1 - E_0)\rho_1^p + E_0 \end{aligned} \tag{15}$$

These design variables indicate the ratio of the material density to the standard density; ρ_{1e} and ρ_{2e} are expressed as $\rho_{1e} = \left(\frac{\rho_{\mathrm{A}e}}{\rho_{\mathrm{A}0}}\right)$ and $\rho_{2e} = \left(\frac{\rho_{\mathrm{B}e}}{\rho_{\mathrm{B}0}}\right)$, where $\rho_{\mathrm{A}e}$ and $\rho_{\mathrm{B}e}$ represent the material densities for materials A and B of the two-phase material, respectively; and $\rho_{\mathrm{A}0}$ and $\rho_{\mathrm{B}0}$ indicate the values of the standard density for materials A and B, respectively. The gradient of the Lagrange function with respect to ρ_{1e} and ρ_{2e} is expressed by Eqs. (16) and (17), respectively. These equations are used to update the design variables.

$$\frac{\partial J^*}{\partial \rho_{1e}} = \boldsymbol{\lambda}_e^T \frac{\partial \boldsymbol{K}_e}{\partial \rho_{1e}} \boldsymbol{u}_e = -\boldsymbol{u}_e^T \frac{\partial \boldsymbol{K}_e}{\partial \rho_{1e}} \boldsymbol{u}_e \quad (16)$$

$$\frac{\partial J^*}{\partial \rho_{2e}} = \boldsymbol{\lambda}_e^T \frac{\partial \boldsymbol{K}_e}{\partial \rho_{2e}} \boldsymbol{u}_e = -\boldsymbol{u}_e^T \frac{\partial \boldsymbol{K}_e}{\partial \rho_{2e}} \boldsymbol{u}_e \quad (17)$$

If the gradients in Eqs. (16) and (17) are directly employed, then a checkerboard-like structure is obtained as the optimized result[5]. Therefore, the filtering method, that is, the sensitivity filter, is generally applied to control the complexity of the structure (Eqs. (18) and (19)). The smoothed gradient values are calculated from $\frac{\partial \overline{J^*}}{\partial \rho_{1e}}$ and $\frac{\partial \overline{J^*}}{\partial \rho_{2e}}$ using the weighting coefficient shown in Eq. (20). The smoothing effect is adjusted to the filtering radius R, and mx indicates the number of elements.

$$\frac{\partial \overline{J^*}}{\partial \rho_{1e}} = \frac{\sum_{e=1}^{mx} w(x_j,y_j) \frac{\partial J^*}{\partial \rho_j} \rho_j}{\rho_{1e} \sum_{e=1}^{mx} w(x_j,y_j)} \quad (18)$$

$$\frac{\partial \overline{J^*}}{\partial \rho_{2e}} = \frac{\sum_{e=1}^{mx} w(x_j,y_j) \frac{\partial J^*}{\partial \rho_j} \rho_j}{\rho_{2e} \sum_{e=1}^{mx} w(x_j,y_j)} \quad (19)$$

$$w(x_j,y_j) = R - \sqrt{(x_j - x_e)^2 + (y_j - y_e)^2} \quad (20)$$

In addition, volume constraint conditions are included in the Lagrange function. The modified Lagrange function is expressed by Eq. (21), where Λ_1 and Λ_2 indicate the adjoint variables, and V_1 and V_2 are the volume constraint conditions. V_1 and V_2 are expressed by Eqs. (22) and (23), respectively; v_e, V_{total}, $\overline{\rho_{1e}^{(0)}}$, and $\overline{\rho_{2e}^{(0)}}$ indicate the volume of each element, the total volume, and the average of design variables ρ_{1e} and ρ_{2e} at the 0th iteration, respectively. In two-dimensional problems, unit thickness is assumed.

$$L = J^* + \Lambda_1 V_1 + \Lambda_2 V_2 \quad (21)$$

$$V_1 = \sum_{e=1}^{mx} \frac{v_e \rho_{1e}}{V_{total}} - \overline{\rho_{1e}^{(0)}} \leq 0 \quad (22)$$

$$V_2 = \sum_{e=1}^{mx} \frac{v_e \rho_{2e}}{V_{total}} - \overline{\rho_{2e}^{(0)}} \leq 0 \quad (23)$$

Design variables ρ_{1e} and $\rho_{2e}$are updated using the optimality criteria method (see Eqs. (24) and (25)), where k and η indicate the number of iterations and the weighting factor, respectively.

$$\rho_{1e}{}^{(k+1)} = \rho_{1e}{}^{(k)} \left(\frac{\left(\frac{\partial \overline{J^*}}{\partial \rho_{1e}}\right)^{(k)}}{-\Lambda_1{}^{(k)} \left(\frac{\partial V}{\partial \rho_{1e}}\right)^{(k)}} \right)^{\eta} \quad (24)$$

$$\rho_{2e}{}^{(k+1)} = \rho_{2e}{}^{(k)} \left(\frac{\left(\frac{\partial \overline{J^*}}{\partial \rho_{2e}}\right)^{(k)}}{-\Lambda_2{}^{(k)} \left(\frac{\partial V}{\partial \rho_{2e}}\right)^{(k)}} \right)^{\eta} \quad (25)$$

The computational flow is illustrated in Fig. 1. In Eqs. (24) and (25), the adjoint variables Λ_1 and Λ_2 are calculated using the bisection method. However, at the final iteration, the computed adjoint variables Λ_1 and Λ_2 are directly used, and the intermediate material is obtained at the junction points of materials A and B. Therefore, at the 7th step shown in Fig. 1, the material separation process is computed. Definitions and examples of the material separation are shown in Fig. 2. The values l_1 and l_2 are computed using the bisection method as well.

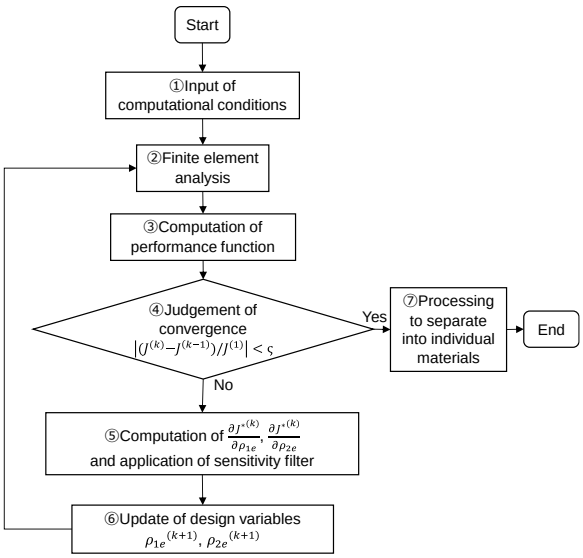

Fig.1 Computational flow.

Definition

$\rho_1 < l_1$ Material A (Absence) $\Longrightarrow$ $\rho_1 = 0$

$\rho_1 \geq l_1$ Material A (Presence) $\Longrightarrow$ $\rho_1 = 1$

$\rho_2 < l_2$ Material B (Absence) $\Longrightarrow$ $\rho_2 = 0$

$\rho_2 \geq l_2$ Material B (Presence) $\Longrightarrow$ $\rho_2 = 1$

Find adjoint variables $\Lambda_1(=l_1)$ and $\Lambda_2(=l_2)$
so as to satisfy the volume constraint condition
under the above definition

⇩ After the above computation

$$E(\rho_1, \rho_2) = (E_2 - E_1)\rho_1^p \rho_2^p + (E_1 - E_0)\rho_1^p + E_0$$

$\rho_1 = 0, \rho_2 = 0 \Longrightarrow E = E_0$

$\rho_1 = 0, \rho_2 = 1 \Longrightarrow E = E_0$

$\rho_1 = 1, \rho_2 = 0 \Longrightarrow E = E_1$

$\rho_1 = 1, \rho_2 = 1 \Longrightarrow E = E_2$

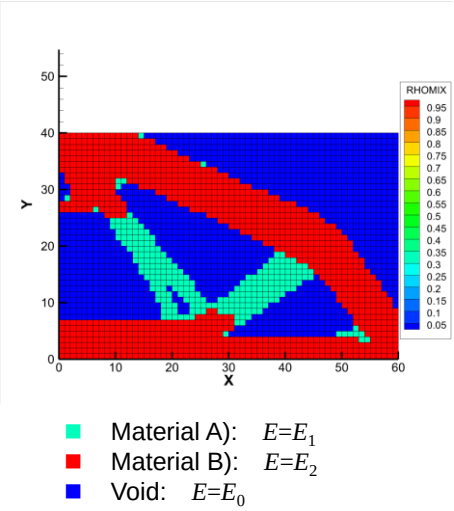

Fig.2 Definition and example of material separation.

3. Numerical experiments

In this study, numerical experiments were performed on the MBB model shown in Fig. 3. The computational conditions are presented in Table 1. The value of the strain energy was compared between the results obtained with and without processing to classify them into individual materials. This investigation was performed by changing the volume reduction rate of material B: Case 1, 60%; Case 2, 70%; Case 3, 80%; and Case 4, 90%. The volume reduction rate of material A was fixed at 50%. Design variables ρ_1 and ρ_2 are the design parameters for materials A and B, respectively.

The numerical results for each case are shown in Figs. 4 and 5. Fig. 4 shows the variation in the performance function for each case, and Fig. 5 shows a comparison of the optimized topologies with and without complete separation of design variables ρ_1 and ρ_2. In Fig. 5, the value of strain energy for each case is shown in the lower row; the result shown on the left is that without the application of the separation process to materials A and B, and the result shown in the right is that with the application. The results show that the value of strain energy in the case with separation is lower than that without separation.

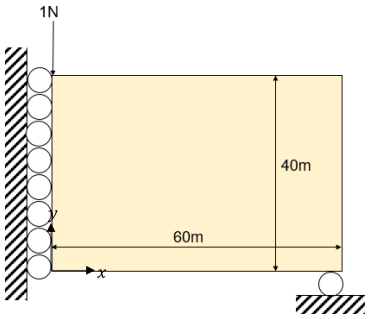

Fig.3 Computational model.

Table 1 Computational conditions.

Total number of elements	2400
Total number of nodes	2501
Mesh size [m]	1
Material A : Young's modulus (E_1) [Pa]	1
Material B : Young's modulus (E_2) [Pa]	2
Poisson's ration ν	0.3
Design domain [m^2]	40×60
Convergence criterion ε	1.0×10^{-5}
Filtering radius R [m]	1.5
Penalty parameter p	3
Weighting factor η	0.75
Move limit of non-dimensional density	0.05

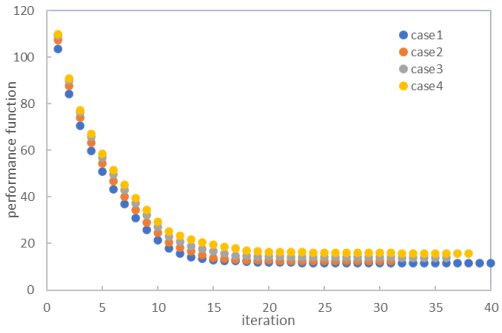

Fig.4 Variation in performance function.
(X-axis: Number of iterations; Y-axis: Strain energy)

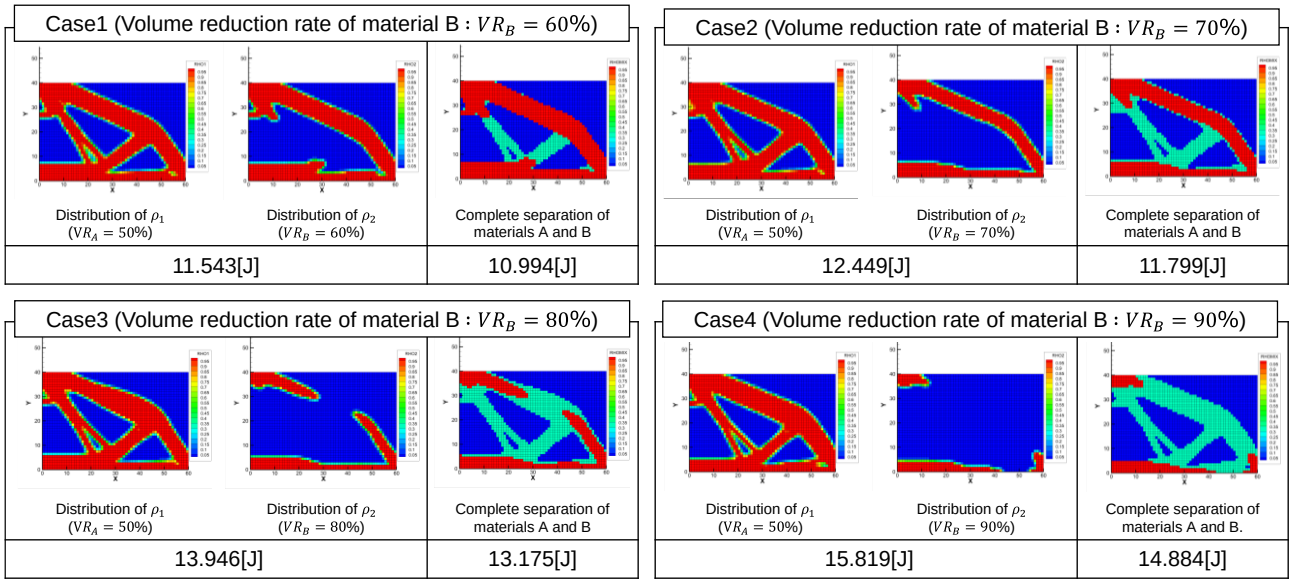

Fig. 5 Comparison of optimized topologies with and without complete separation of design variables ρ_1 and ρ_2.

4. Conclusions

In this study, numerical experiments involving maximally stiff structure problems using two-phase materials were performed via density-based topology optimization, and the strain energy was compared for cases with and without separation for two-phase materials. The MBB model was employed in the computational model. Results showed that the strain energy of the optimized result with separation for the two-phase material was lower than that without separation.

Notably, we previously developed a new update method for the design parameter[6]. In the future, we intend to apply the method to the present study.

Acknowledgements: The computations were performed using computer facilities at Kyushu University's Research Institute for Information Technology. We wish to thank the staff at Kyushu University's Research Institute for Information Technology. We would like to thank Editage (www.editage.com) for English language editing.

References

1) Nikkei Business Publications, Inc. from < https://xtech.nikkei.com/atcl/nxt/column/18/01516/00004/ >, (accessed on 4 January, 2023). (in Japanese)
2) JFE Steel Corporation from <https://www.jfe-steel.co.jp/release/2019/01/190109.html >, (accessed on 4 January, 2023). (in Japanese)
3) Y. Wada, T. Yamamoto, K. Yuge, A. Nakamoto, I. Kizaki and M. Ueno : *Multiphase Topology Optimization under Various Mix Conditions*, Transactions of the Society of Automotive Engineers of Japan, Vol.49, No.2, pp.329-334, 2018. (In Japanese.)
4) M. Kawahara : *Finite element methods in incompressible, adiabatic, and compressible flows*. Springer, 2016.
5) S. Nishiwaki, K. Izui and N. Kikuchi: *Topology optimization*, Maruzen Publishing Co.,Ltd., 2013. (In Japanese.)
6) M. Kishida and T. Kurahashi : *Proposal of a modified optimality criteria method for topology optimization analysis in 3-dimensional dynamic oscillation problems*, International Journal for Numerical Methods in Engineering, Vol.123, Issue3, pp.866-896, 2022.

(Received July 19, 2023)